Circular Electric Mode Directional Coupler*

BUNICHI OGUCHI†, SENIOR MEMBER, IRE

Summary—**This paper describes a circular electric mode directional coupler, composed of two coaxial bifurcations in circular waveguide. The coupling coefficient of the directional coupler depends on the separation between the two bifurcations, and a hybrid junction for the circular electric mode may be obtained at the proper separation. The analysis is carried out in terms of scattering matrix elements characterizing each coaxial bifurcation.**

The scattering matrix elements were experimentally determined via the Weissfloch tangent method at 5000-Mc band. For convenience, experiments were carried out in sectoral waveguide instead of circular waveguide. Measured characteristics at 9000-Mc band are in good agreement with values determined by circuit calculations employing parameters of the coaxial bifurcation measured at 5000-Mc band. For the case of a hybrid junction, wide-band matching has been accomplished and verified experimentally. Applications of this directional coupler are outlined.

Introduction

THE circular electric mode has received a great deal of attention, especially in connection with millimeter waves, because of its low-loss transmission characteristics. There have been many publications about TE_{01} mode transducers which transfer power from the dominant mode in rectangular waveguide to the TE_{01} mode in circular waveguide. With the exception of the mode transducer, however, there has been little information about circular electric mode components whose design is complicated by the fact that even a small discontinuity in circular waveguide easily gives rise to spurious modes.

This paper describes a symmetrical directional coupler involving the circular electric mode, composed essentially of two coaxial bifurcations in a circular waveguide. (Cf. Figs. 1 and 4.) Consider a circular waveguide in which the TE_{01} and TE_{02} modes can propagate, but the TE_{03} mode is beyond cutoff. A coaxial bifurcation is located at the special surface on which $E_\phi = 0$ for the TE_{02} mode. In this bifurcated region, only one of the two circular electric modes can propagate in the small circular waveguide and the coaxial waveguide, respectively.[1]

Suppose two separate coaxial bifurcations to be located in a circular waveguide. If a circular electric mode is incident into the circular waveguide region from one of the bifurcated regions, the TE_{01} and TE_{02} modes are simultaneously excited in the circular waveguide region. These TE_{01} and TE_{02} modes have differing phase velocities. Because of this difference, the phase relation between the two modes changes along the waveguide, and the two modes interfere with one another. In the second bifurcated region, they excite respective circular electric modes whose amplitudes are changed by the phase difference between the TE_{01} and TE_{02} modes at the second bifurcation. Therefore, a wide variety of transfer coefficients between the two four-ports may be obtained by changing the separation between the bifurcations. In particular, a hybrid junction may be obtained at the proper separation. These characteristics are very similar to those of the short-slot hybrid junction in rectangular waveguide.[2]

The circuit parameter of a bifurcation in a circular waveguide was determined, experimentally, through the Weissfloch tangent method at 5000-Mc band. A directional coupler has been constructed at 9000-Mc band in sectoral waveguide, instead of circular waveguide, for the sake of experimental convenience. Measured characteristics of this directional coupler are in good agreement with values determined by circuit calculations employing parameters of the coaxial bifurcation measured at 5000-Mc band. For a hybrid junction, wide-band matching has been accomplished and verified experimentally.

Hybrid junctions may be employed to realize a branching filter for a TE_{01} mode transmission system. A TE_{01}-TE_{02} mode transducer in a circular waveguide may be constructed by utilizing this directional coupler.

Coaxial Bifurcation of a Circular Electric Mode Waveguide

A. General Characteristics

We shall consider characteristics of a coaxial bifurcation of a circular waveguide by a circular cylindrical partition of zero thickness. In region I, shown in Fig. 1, a cylinder partitions a circular waveguide into a small circular waveguide and a coaxial waveguide. Each waveguide has its own circular electric mode. The ratio of the diameter D_1 of the cylindrical partition to the diameter D_2 of the circular waveguide is chosen such that $D_1/D_2 = x_{01}'/x_{02}'$, where x_{01}' and x_{02}' are, respectively, the first and second nonzero roots of

* Received by the PGMTT, May 20, 1960; revised manuscript received, August 22, 1960. The work described in this report was performed at the Microwave Res. Inst., Polytechnic Institute of Brooklyn, Brooklyn, N. Y., under Contract No. DA-36-039 sc-78001 sponsored by the USASRDL.

† Electrical Communication Lab., Nippon Telegraph and Telephone Public Corp., Tokyo, Japan.

[1] Inherent in the construction of this junction is circular symmetry; thus, the TE_{01} mode excites only TE_{0n} mode ($n = 1, 2 \cdots$), and the junction may be represented by a four-port circuit. But this picture changes if another mode is employed in this junction.

A similar consideration can be employed for the TM_{0n} modes in such a bifurcated waveguide, but here we will only deal with the TE_{0n} modes.

[2] H. J. Riblet, "The short-slot hybrid junction," PROC. IRE, vol. 40, pp. 180–184; February, 1952.

$J_0'(x)=0$. This special location of the cylindrical partition coincides with a surface $E_\phi=0$ for the TE_{02} mode in the circular waveguide. Region II is a circular waveguide in which both the TE_{01} and TE_{02} modes can propagate, and the TE_{03} mode is beyond cutoff.

Suppose the TE_{02} mode to be incident from the circular waveguide on the left in Fig. 1. This mode can propagate towards the right in region I without any disturbance by the partition because of the special choice of the diameter of the cylindrical partition. The incident power is divided between the lowest cutoff circular electric mode in the smaller circular waveguide, and the lowest cutoff coaxial circular electric mode in the coaxial waveguide in region I. This power ratio is easily calculated from the field distribution of the circular TE_{02} mode. On the other hand, if the TE_{01} mode is incident from the left, a small amount of power is reflected from the end of the partition; the remainder is divided between the two modes mentioned above. Even in this case, no other mode is generated far from the edge of the bifurcation except these three modes, because the whole construction is circularly symmetric. The reflected power remains only in the same circular TE_{01} mode, and no TE_{02} mode is generated in region II. The latter is easily seen to follow from reciprocity and the fact that the incident TE_{02} mode suffers no reflection.

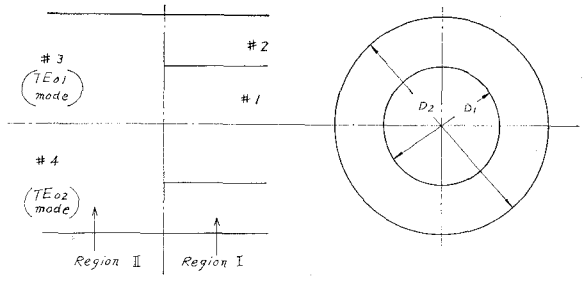

Fig. 1—Coaxial bifurcation of a circular waveguide.

Let us express these relations more clearly by using scattering matrix notation. We label the TE_{01} mode port of the small circular waveguide on the right port no. 1, the right coaxial mode port no. 2, the large circular TE_{01} mode port on the left no. 3, and the circular TE_{02} mode port on the left no. 4, as shown in Fig. 1. All metallic walls are assumed to be perfectly conducting. The important points are that, as demonstrated in the preceding paragraph, $s_{34}=s_{44}=0$, where s_{ij} are the scattering matrix elements. Because of this fact and the unitary condition on the scattering matrix, all magnitudes of the scattering coefficients may be expressed rigorously in terms of the two parameters $|s_{14}/s_{24}|=k$ and $|s_{33}|=r$, where k is an amplitude ratio of transmission coefficients of the TE_{02} mode between two coaxial waveguides, and r is a magnitude of a reflection coefficient of the TE_{01} mode in a large circular waveguide. The expressions are as follows:

$$|s_{11}|=\frac{r}{1+k^2},\quad |s_{12}|=\frac{kr}{1+k^2},\quad |s_{13}|=\frac{\sqrt{1-r^2}}{\sqrt{1+k^2}},$$

$$|s_{14}|=\frac{k}{\sqrt{1+k^2}},\quad |s_{22}|=\frac{k^2r}{1+k^2},\quad |s_{23}|=\frac{k\sqrt{1-r^2}}{\sqrt{1+k^2}},$$

$$|s_{24}|=\frac{1}{\sqrt{1+k^2}},\quad |s_{33}|=r,\quad |s_{34}|=|s_{44}|=0. \qquad (1)$$

Also, we may get the following relations among the phasors of the scattering coefficients by the same considerations. Denote the phase angle of s_{ij} by ϕ_{ij}, then

$$\begin{aligned}\phi_{11}&=\phi_{22}=\phi_{12}\pm 2m\pi,\\ \phi_{13}&=\phi_{23},\\ \phi_{14}&=\phi_{24}\pm\pi,\ \text{and}\\ \phi_{11}+\phi_{33}&=2\phi_{13}\pm(2m'+1)\pi,\end{aligned} \qquad (2)$$

where m and m' are integers.

The value of k, computed from the field configuration of the TE_{02} mode, is 1.077. Also, the value of ϕ_{14} is easily determined because no field disturbance of the TE_{02} mode occurs at the end of the bifurcation. Upon choosing the boundary plane between regions I and II as the reference plane for all ports, ϕ_{14} becomes 0. Therefore, if we could obtain the values of r, ϕ_{33} and ϕ_{13} by some means, the whole scattering matrix characterizing this bifurcation would be determined by (1) and (2).

B. Measured Parameters

As indicated in the previous section, the problem of obtaining the scattering matrix of the bifurcation is reduced to the problem of getting the values of r, ϕ_{33} and ϕ_{13}. We have decided to measure these values experimentally. The Weissfloch tangent method for the TE_{01} mode has been employed for the analysis of a resonance type measurement. The measurements have been carried out in a circular waveguide of 5.758 inches ID at 5000-Mc band of frequencies. A conducting cylindrical partition of 3.145-inch mean diameter and 0.005-inch thickness is supported concentrically inside the circular waveguide by a polyfoam annulus of 1-inch length. A polyfoam pill box of the same length is inserted in a corresponding position inside the cylindrical partition, in order to keep the same phase constant in both the inside and outside regions of the partition cylinder. The circular waveguide is closed at both ends by movable plungers to form a resonant cavity, as shown in Fig. 2.

The cavity is equipped with exciting and detecting magnetic probes. A mode absorbing filter for TE_{0n} mode composed of polyfoam and radial resistive cards is used to eliminate effects of the spurious modes. In the frequency range of interest many spurious resonances may occur, since the operating frequency is so high that the TE_{02} mode can also propagate.

The usual Weissfloch tangent method may be applied to the measurement of one discontinuity. In our case, however, as shown in Fig. 2, the discontinuity of interest for the TE_{01} mode occurs twice, at both ends of the bifurcated region consisting of circular and coaxial waveguides, isolated from each other. Although different amplitudes of respective modes are excited in both waveguides by the incident TE_{01} mode, these two waves suffer the same amount of phase shift at the end of the bifurcation, as shown in (2), and have the same phase velocity in the respective waveguides; moreover, the TE_{01} mode does not couple to the TE_{02} mode at the discontinuities, located at both ends of the bifurcated region. Thus, these two waves may be considered as one normal mode in the two waveguides, and for the purpose of determining the three parameters, r, ϕ_{33}, and ϕ_{13}, the bifurcated region may be represented by one equivalent line connected between the discontinuities. Then, the Weissfloch tangent method gives us the characteristics of the whole circuit, comprising the two symmetrically placed discontinuities and a length of waveguide. Since this circuit has a symmetrical character, with respect to the central plane of this region, these over-all characteristics may yield only two independent parameters.

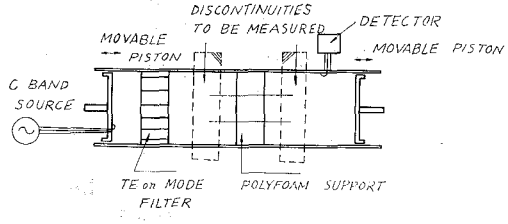

Fig. 2—Measuring cavity.

It is necessary, however, to have three independent parameters in order to determine the three parameters, r, ϕ_{33}, and ϕ_{13}. Some further measurement is required. If we measure the circuit again, changing only the length of the bifurcated region, we again obtain two parameters. Then, we may determine the desired circuit parameters from the four values and the known changed length of the bifurcated region. Actually, we have employed three cylindrical partitions of different lengths, nominally 2 inches, $2\frac{1}{2}$ inches, and 3 inches. (Actual lengths are 2.032 inches, 2.513 inches, and 3.044 inches, respectively.)

The equations relating the desired parameters of the bifurcation to these measured parameters may be conveniently determined by expressing every portion of the circuit in the form of a scattering transfer matrix, because the bifurcated region may be expressed by one line for this purpose, as mentioned before.

Even though polyfoam has a dielectric constant similar to that of air, it is better to treat it as a distinct portion, and thereby compensate for any effect caused by polyfoam. We have measured the dielectric constant of polyfoam by the Weissfloch tangent method in the same circular waveguide for the TE_{02} mode. This constant has been 1.027, which has been employed to compensate for the polyfoam effect.

We have measured the various coaxial bifurcations with different lengths by the above method at four different frequencies within 5000-Mc band. The scattering transfer matrix elements of the bifurcation may be calculated from the measured values by compensating for the polyfoam effect. In this calculation, each element is expressed in a form $T_{ij}=T_{ij0}+t_{ij}$, where T_{ij0} is an element obtained by neglecting the effect of polyfoam. The t_{ij} may be determined by a successive approximation method to first order in $\epsilon-1$, where ϵ is a relative dielectric constant of polyfoam.

The parameters of the coaxial bifurcation for the TE_{01} mode may be obtained from the calculated matrix elements. Frequency characteristics of r, ϕ_{33} and ϕ_{13} are shown in Fig. 3. In this figure, 9000-Mc band frequency is also indicated as the abscissa for convenience in later application, where $a=\frac{1}{2}D_2$.

These parameters are expected to have a character similar to the analogous parameters for an H-plane $0°=Y$ junction of a wide rectangular waveguide, because the field configurations for both cases are similar.[3]

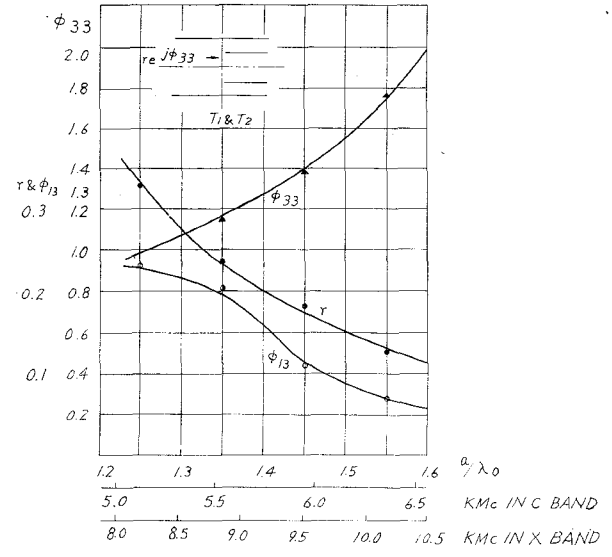

Fig. 3—Frequency characteristics of r, ϕ_{33}, and ϕ_{13}. All reference planes are on the boundary plane of the bifurcation.

Circular Electric Mode Directional Coupler

A. General Characteristics

Let us consider the characteristics of a circular electric mode directional coupler composed of the above mentioned bifurcations, which are located symmetrically along an axis, as shown in Fig. 4. If the separation L is sufficiently large to neglect the interaction

[3] N. Marcuvitz, "Waveguide Handbook," Mass. Inst. Tech., Rad. Lab. Ser., McGraw-Hill Book Co., Inc., New York, N. Y., vol. 10, p. 383; 1951.

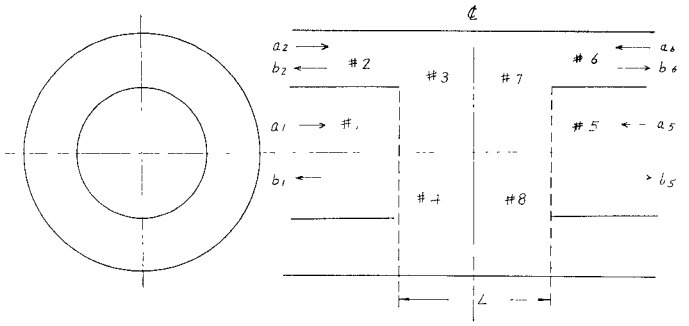

Fig. 4—Circular electric mode directional coupler.

effect caused by cutoff between the two bifurcations, relations between the incident, reflected, and transmitted waves are easily expressed in terms of the scattering matrix elements of each bifurcation, and phase delays engendered by the separation. When the concealed ports are eliminated, the scattering matrix for the over-all coupler network, shown in Fig. 4, are as follows:

$$\begin{pmatrix} b_1 \\ b_2 \\ b_5 \\ b_6 \end{pmatrix} = S \begin{pmatrix} a_1 \\ a_2 \\ a_5 \\ a_6 \end{pmatrix} \qquad S = \begin{pmatrix} S_{11} & S_{12} & S_{15} & S_{16} \\ S_{21} & S_{22} & S_{25} & S_{26} \\ S_{51} & S_{52} & S_{55} & S_{56} \\ S_{61} & S_{62} & S_{65} & S_{66} \end{pmatrix} \tag{3}$$

$$S_{11} = S_{55} = s_{11} + \frac{s_{13}^2 s_{33}}{\eta} e^{-j2\theta_3} = \frac{re^{j\phi_{11}}}{1+k^2} \frac{1 - e^{-j2(\theta_3 - \phi_{33})}}{\eta}$$

$$S_{12} = S_{56} = s_{12} + \frac{s_{13} s_{23} s_{33}}{\eta} e^{-j2\theta_3} = kS_{11}$$

$$S_{22} = S_{66} = s_{22} + \frac{s_{23}^2 s_{33}}{\eta} e^{-j2\theta_3} = k^2 S_{11}$$

$$S_{15} = \frac{s_{13}^2}{\eta} e^{-j\theta_3} + s_{14}^2 e^{-j\theta_4} = \frac{e^{-j\theta_4}}{1+k^2}\left[\frac{1-r^2}{\eta} e^{-j\Theta} + k^2\right] \tag{4}$$

$$S_{16} = S_{25} = \frac{s_{13} s_{23}}{\eta} e^{-j\theta_3} + s_{14} s_{24} e^{-j\theta_4}$$

$$= \frac{ke^{-j\theta_4}}{1+k^2}\left[\frac{1-r^2}{\eta} e^{-j\Theta} - 1\right]$$

$$S_{26} = \frac{s_{23}^2}{\eta} e^{-j\theta_3} + s_{24}^2 e^{-j\theta_4} = \frac{e^{-j\theta_4}}{1+k^2}\left[\frac{k^2(1-r^2)}{\eta} e^{-j\Theta} + 1\right]$$

$$\eta = 1 - s_{33}^2 e^{-j2\theta_3} = 1 - r^2 e^{-j2(\theta_3 - \phi_{33})}$$

$$\theta_3 = \beta_3 L, \qquad \theta_4 = \beta_4 L$$

$$\Theta = \theta_3 - \theta_4 - 2\phi_{13}, \tag{5}$$

where

a_1, a_2, a_5, a_6 = the incident wave phasors in the circular and coaxial waveguides, respectively, (Fig. 4)

b_1, b_2, b_5, b_6 = the reflected wave phasors in the circular and coaxial waveguides, respectively, (Fig. 4)

β_3 = the propagation constant of the TE_{01} mode in the larger circular waveguide, and

β_4 = the propagation constant of the TE_{02} mode in the larger circular waveguide.

It is evident that there is a simple relation between S_{11}, S_{12}, and S_{22}, and that these three values are almost the same because k is very close to unity. The magnitudes of these values are always small because r is small. On the other hand, the magnitudes of S_{15}, S_{16} and S_{26} vary widely between 0 and 1, depending upon the phase difference Θ.

There are two conditions for no reflection and infinite directivity. One is that $\theta_3 - \phi_{33} = n\pi$ (n: integer), and the other is that r is cancelled by employing some additional matching element which has no effect on the TE_{02} mode. The former condition is rather complicated in design, because θ_3 is also linearly dependent on Θ, which is fixed mainly by the specified transfer coefficient. Moreover, this method may be frequency sensitive, because, although the variation of ϕ_{33} tends to compensate for the variation of θ_3, θ_3 changes quickly with frequency. As we will explain later, the latter condition may be expected to yield wide-band characteristics.

For either of the above ideal conditions, we have the following relations from (3), (4) and (5):

$$S_{11} = S_{12} = S_{22} = S_{55} = S_{56} = S_{66} = 0,$$

$$S_{15} = \frac{e^{-j\theta_4}}{1+k^2}\left[k^2 + e^{-j\Theta}\right],$$

$$S_{16} = S_{25} = \frac{-ke^{-j\theta_4}}{1+k^2}\left[1 - e^{-j\Theta}\right],$$

$$S_{26} = \frac{e^{-j\theta_4}}{1+k^2}\left[1 + k^2 e^{-j\Theta}\right]. \tag{6}$$

A vector diagram of S_{15}, S_{16}, S_{25} and S_{26} is shown in Fig. 5. As illustrated in this figure, the magnitudes of S_{15} and S_{26} are the same. The phase angles between S_{16} (or S_{25}), S_{15} and S_{26} are not $\pi/2$, as in the analogous rectangular waveguide short-slot junction, but $\pi/2 \pm (\Theta/2 - \alpha)$ respectively, where

$$\alpha = \sin^{-1} \frac{\sin\Theta}{\sqrt{1 + 2k^2\cos\Theta + k^4}}.$$

However, as k is very close to unity (actually 1.077), $(\Theta/2 - \alpha)$ is a small quantity. The magnitudes of S_{15}, S_{16}, S_{25} and S_{26} are widely changed by Θ. If Θ becomes $2n\pi$ (n: integer), $S_{16} = S_{25} = 0$ and $|S_{15}| = |S_{26}| = 1$. Nevertheless, S_{15} and S_{26} may not vanish completely, even though a very small minimum value of 0.0745 (−22.6 db) occurs at $\Theta = (2n+1)\pi$. If Θ is chosen to be

$$\Theta = (2n+1)\pi \mp \mathrm{Cos}^{-1} \frac{(k^2-1)^2}{4k^2} = 90.32°, 269.68°, \cdots,$$

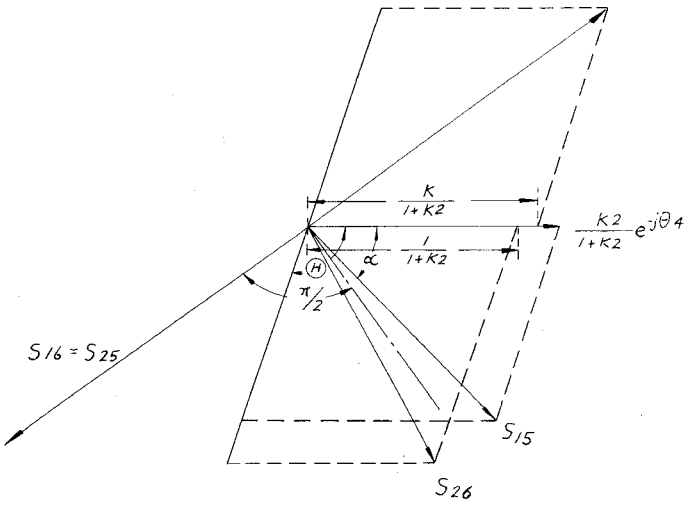

Fig. 5—Vector diagram of S_{15}, S_{16}, S_{25} and S_{26}.

then

$$|S_{15}| = |S_{16}| = |S_{25}| = |S_{26}| = \frac{1}{\sqrt{2}},$$

and the coupler becomes a 3-db hybrid coupler.

B. Measured Characteristics

Experiments on this directional coupler have been carried out at 9000-Mc band within sectoral waveguide instead of circular waveguide. The principle is not changed by using sectoral waveguide, and then a very simple rectangular to sectoral waveguide taper operates as a required mode transducer. Furthermore, it is not necessary to worry about spurious modes in such a transducer, if the sector angle is chosen properly. The experimental setup is composed of H-plane branched waveguides, rectangular to sectoral taper waveguides and a directional coupler portion as is illustrated in Fig. 6. The sector angle is chosen as 22.5° in order to render the mode equivalent to the circular TE_{71} mode nonexistent in the sectoral guide. Rectangular waveguides at both ends have the conventional dimension of 0.9 inch×0.4 inch so that ordinary components for the 9000-Mc band may be employed. Other dimensions are shown in Fig. 6. The taper waveguides, which have been made by electroforming, are rather long to reduce reflection. The directional coupler portion has been constructed by assembling brass blocks and an interchangeable partition plate of 0.005-inch thickness between them. This permits us to change the dimensions of the coupling region very easily, during experiments.

Frequency characteristics of the measured magnitudes of the transfer coefficients for the directional coupler are shown in Fig. 7. We have measured the transfer coefficient S_{12} between adjoining ports instead of the reflection coefficients S_{11} and S_{22}, because they are proportional, as shown in (4). Calculated values which are obtained from (4) and (5) using values of the parameters, r, ϕ_{33} and ϕ_{13}, measured at 5000-Mc band

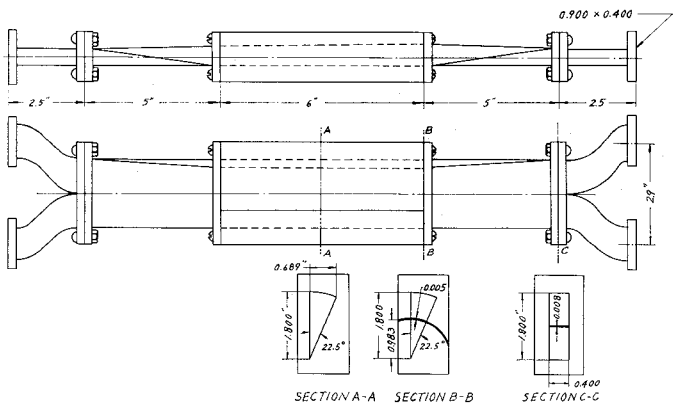

Fig. 6—Experimental setup of the directional coupler.

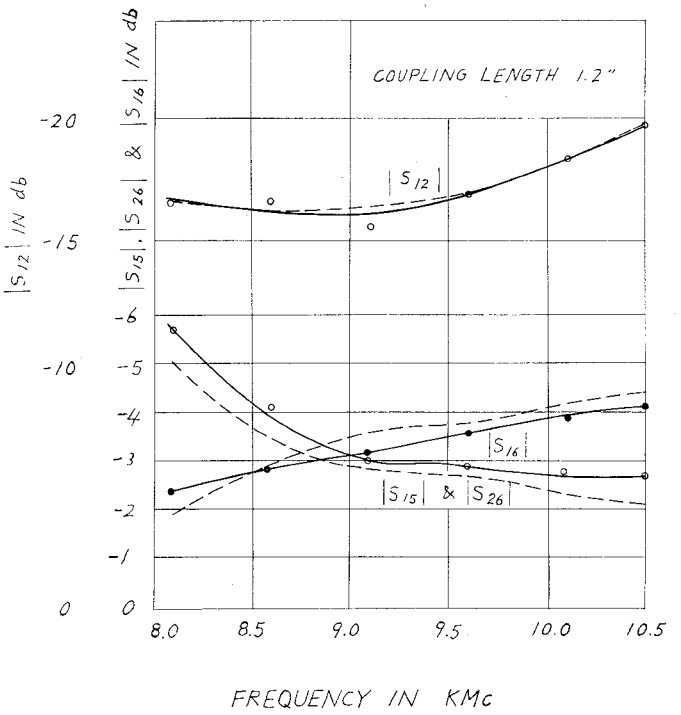

Fig. 7—Frequency characteristics of transfer coefficients for the directional coupler.
———— measured curve,
– – – – – calculated curve.

in Fig. 3, are also shown on the same graphs. The magnitudes of the same transfer coefficients vs the coupling length are shown in Fig. 8. The measured values, in both cases, are in good agreement with calculated ones. The fact that the difference between measured and calculated values increases as the coupling length becomes short is thought to be a result of cutoff mode interaction between bifurcations, which is neglected in the calculation. $|S_{15}|$ and $|S_{26}|$ are, in general, not distinguishable in these figures, unless the reflection coefficient becomes quite large or $|S_{15}|$ becomes very small.

As illustrated in Fig. 7, the variations of $|S_{15}|$ and $|S_{16}|$ with frequency are rather small. This is attributed to the fact that variations of $(\theta_3 - \theta_4)$ and ϕ_{13} have

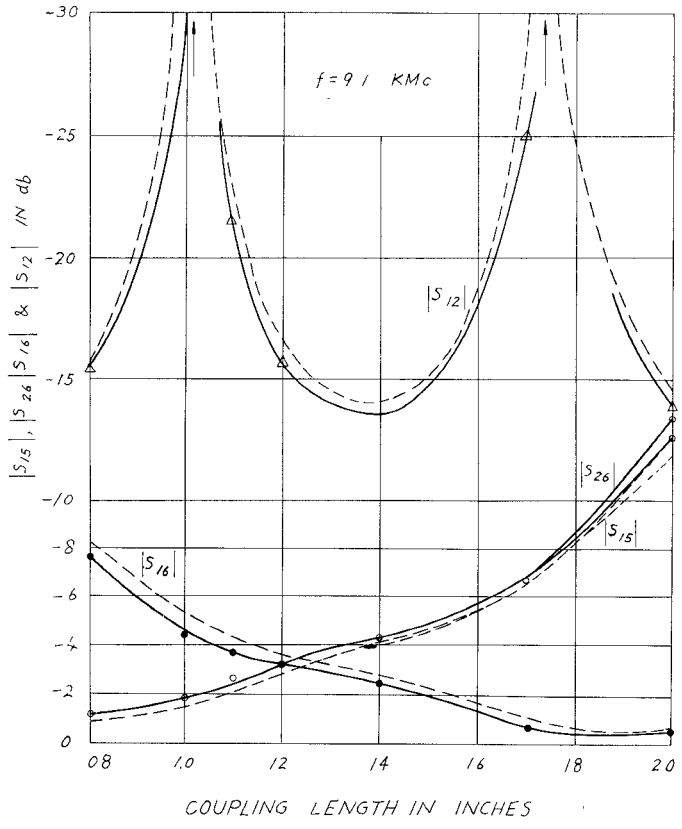

Fig. 8—Transfer coefficients vs coupling length characteristics.
———— measured curve,
– – – – – calculated curve.

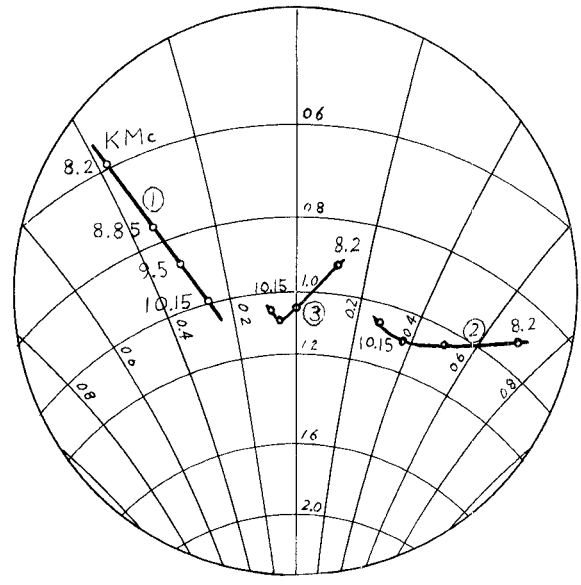

Fig. 9—TE_{01} mode admittance characteristics of the coaxial bifurcation, seen from the circular waveguide.
① refers to the boundary plane,
② refers to the plane 0.365 inch apart from the boundary plane, and
③ refers to the addition of a strip of 0.04 inch width.

the same trend with frequency, as shown in Fig. 3. Then the variation of Θ becomes small. Thus, we may expect a wide-band component if we utilize these characteristics properly.

As mentioned before, there are two methods for reducing the reflection coefficient. The method which cancels S_{33} by some matching element is better than the other in all respects. The TE_{01} mode admittance characteristics of the bifurcation, seen from the circular waveguide and referred to the boundary plane, may be obtained from Fig. 3 and have been replotted on a Smith chart, as shown on curve 1 in Fig. 9. In transforming admittances along the guide by rotation about the center of a Smith chart, a given physical length of guide represents more rotation on the chart at higher frequencies than it does at lower ones. Therefore, if the admittances represented by curve 1 are transformed properly along the guide towards the generator, the admittances at all frequencies may fall near the curve of unity conductance on the chart. These transformed characteristics are shown on curve 2 in Fig. 9, in which the physical length of the guide of 0.365 inch is selected, and higher order mode effect, caused by the bifurcation, is assumed to be neglected. These characteristics show that the addition of a shunt susceptance element placed at this referred position gives wide-band matching, if the susceptance has smaller value at higher frequencies than at lower ones. An inductive susceptance has this character.[4] Thus, a thin-strip matching element (same thickness as the partition) with finite width in the axial direction, located on the same cylindrical surface as the bifurcation, may be used for the matching element, because the strip has an inductive susceptance for the TE_{01} mode and no appreciable effect on the TE_{02} mode. The susceptance may be calculated approximately.[5] With the addition of a strip of 0.04-inch width at that position, the input admittances of the bifurcation move into the area around the center on the chart, as shown on curve 3 in Fig. 9. This figure explains the possibility of wide-band matching.

Actually, it was necessary to determine, experimentally, the optimum position for the matching element, because the effective length between the edge of the bifurcation and a matching element might be influenced by the higher modes generated in the vicinity of bifurcation. The optimum length found was considerably shorter than the calculated one, and was 0.286 inch. The matching strips actually used were of the same dimension as the calculated ones.

Another important point is that a matching element causes a phase shift of the transmitted wave in the TE_{01} mode. Suppose a shunt susceptance of B/Y_0 would cancel reflections completely; then the additional phase shift of the transmitted wave caused by the shunt element is given by $\tan^{-1}(-B/2Y_0)$. Thus,

[4] The usual short-slot hybrid junction has a character similar to this coupler. Therefore, it would probably be better to use an inductive element in that case also rather than the capacitive one, which has been commonly used. (See footnote 2.)
[5] Marcuvitz, *op. cit.*, p. 257.

if inductive matching elements are employed, it is necessary to make the coupling length longer, in order to get the same transfer coefficient as previously obtained without a matching element.

The measured magnitudes of the transfer coefficient for a directional coupler are shown in Fig. 10. The coupling length has been chosen with an aim towards obtaining a hybrid junction. It is evident in this figure that, with the inductive matching elements, the magnitude of $|S_{12}|$ becomes quite small in a wide frequency region. Since the taper waveguides, bends, and terminations at the output ports have small reflections, these effects upon $|S_{12}|$ may not be negligible, if $|S_{12}|$ becomes very small. [It has been confirmed that the VSWR of the terminations are less than 1.03 (return loss = 36.6 db) in the entire frequency region of interest.] Nevertheless, it is clear that wide-band match has been obtained, and that the inductive matching elements were quite suitable for this purpose. Also, we were able to get a 3-db hybrid coupler at the center frequency with dimensions of the coupling region as shown in the upper right of Fig. 10. The transfer coefficients S_{15}, S_{26} and S_{16} also have fairly wide-band character. The calculated values shown in the same figure are obtained from (6), taking into account the phase shift caused by matching elements, which is determined by the calculated susceptance value. The calculated and measured values are in very good agreement with one another.

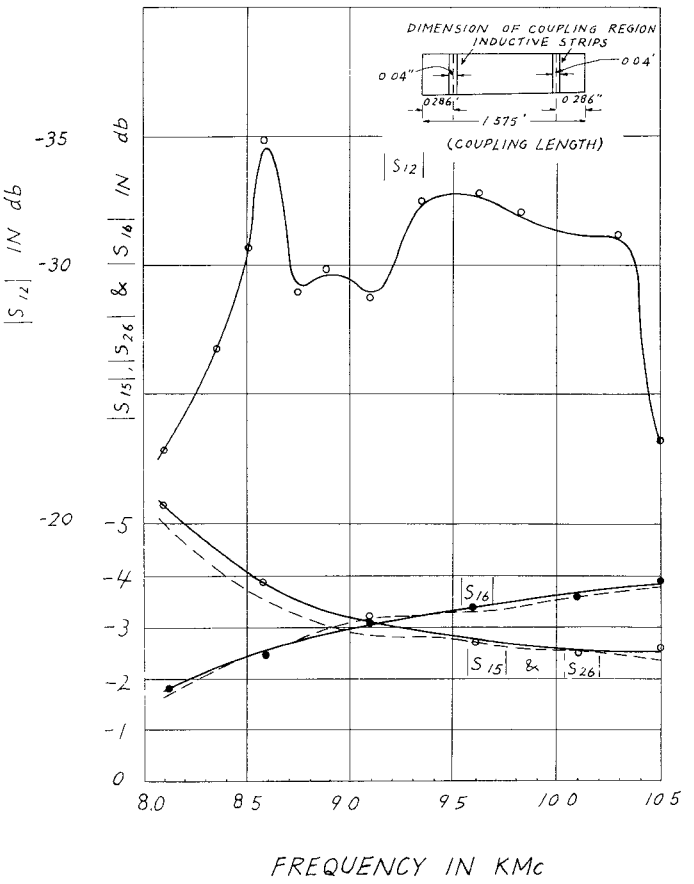

Fig. 10—Frequency characteristics of transfer coefficients for a hybrid junction with inductive matching elements.
——— measured curve,
– – – – – calculated curve.

Applications

Finally, some applications of this directional coupler are described briefly.

These couplers may be used as the important elements of a branching filter for the TE_{01} mode, together with two rejection filters, which are coupled inner and outer waveguides between two couplers, respectively.[6] In this case the coupler in a semicircular waveguide may be employed conveniently.

Another application is a TE_{01}-TE_{02} mode transducer. If we choose the ratio of $|S_{15}|$ to $|S_{16}|$ equal to k, and the phase shift between S_{15} and S_{16} equal to π, then the output waves have the same field configuration as that of TE_{02} mode. The required conditions may be attained by a proper coupling length for the coupler

$$\left(\Theta = \cos^{-1}\frac{k^2 - 1}{2k^2} = 86.0°\right)$$

and the phase shifter. The TE_{01} mode incident in a smaller circular input waveguide is transferred to the TE_{02} mode in a larger circular output waveguide.

[6] W. D. Lewis and L. C. Tillotson, "A non-reflecting filter for microwaves," *Bell Sys. Tech. J.*, vol. 27, pp. 83–95; January, 1948.

Acknowledgment

The author wishes to express his sincere gratitude to Drs. L. B. Felsen and W. K. Kahn for their valuable suggestions, stimulating discussions, and revisions of the manuscript. The author also thanks the staff members of the Electrophysics Group of MRI for their encouragement.